Journal of Chromatography A, 1218 (2011) 5858–5866

Contents lists available at ScienceDirect

Journal of Chromatography A

journal homepage: www.elsevier.com/locate/chroma

Assessment for the light-induced *cis–trans* isomerization of rhapontigenin and its glucoside rhaponticin by capillary electrophoresis and spectrometric methods

Yang Hui[a,b], Xi Li[a,b], Xingguo Chen[a,b,c,*]

[a] National Key Laboratory of Applied Organic Chemistry, Lanzhou University, China
[b] Department of Chemistry, Lanzhou University, Lanzhou 730000, China
[c] Key Laboratory of Nonferrous Metal Chemistry and Resources Utilization of Gansu Province, Lanzhou 730000, China

ARTICLE INFO

Article history:
Received 12 February 2011
Received in revised form 17 June 2011
Accepted 26 June 2011
Available online 3 July 2011

Keywords:
Rhapontigenin
Rhaponticin
UV-induced isomerization
Capillary electrophoresis-diode array detector
UV–vis spectroscopy
NMR spectroscopy

ABSTRACT

The light-induced *cis–trans* isomerization of rhapontigenin (RHA) and its glucoside rhaponticin (RHA-Glc) were evaluated under ultraviolet (UV) light irradiation. A simple and rapid capillary electrophoresis method was developed for the kinetic study of four stilbenes (both *cis* and *trans* form of RHA and RHA-Glc). These analyses were achieved by using β-cyclodextrin (β-CD) modified capillary zone electrophoresis with diode array detector (CZE-DAD). The method provided reliable separations with a short analysis time of 3 min. The purity of individual compound was checked by UV spectral comparisons with known standards, and further confirmed by ^{1}H and ^{13}C nuclear magnetic resonance (NMR) spectroscopy. Furthermore, the UV absorbance and the molar absoptivity (ε) values were determined by UV–vis spectrophotometer to be 36824 L mol^{-1} cm^{-1} at λ_{max} 324.5 nm for *trans*-RHA and 43894 L mol^{-1} cm^{-1} at λ_{max} 325 nm for *trans*-RHA-Glc in methanol/water mixture solution (50%, v:v), respectively. CZE, UV–vis and NMR spectroscopy studies provided similar conclusions by considering the influence of irradiation time and the influence of irradiation wavelength.

1. Introduction

The stilbenes, which are abundant in the plant kingdom, are of recent interest due to their diverse biological profiles. Amongst these, rhapontigenin (RHA) and its glucoside rhaponticin (RHA-Glc) (Fig. 1), phytoalexins belonging to the stilbene subgroup of polyphenols, present in Rhubarb and other Chinese herbal medicine. They have been reported not only to exhibit antithrombotic, antiallergic properties and attenuate cardiac hypertrophy but also exert a protective effect against ethanol-induced liver damage [1–5]. It is worth noting that the stereochemical structures of stilbenes are very important for their activities. For instance, resveratrol (3,5,4′-trihydroxystilbene, RES), just the *trans*-isomers showed the activities of anti-tumour, anti-inflammatory, antioxidant and anti-platelet aggregation [6–12].

On the other hand, stilbenes are extremely photo-sensitive and function in both *cis*- and *trans*-isomeric forms in a number of plant species (Fig. 1) [13–24]. The *trans* form is susceptible to UV-induced isomerization, and is converted to a physiologically considerably less active *cis* form by irradiation for a while. So the UV-induced even ambient light induced isomerization may cause the inactivation of these potential therapeutic agents for humans.

Prior to evaluate any isomerization, information about various isomeric products and by-products must be assessed, in order to determine the yields of the isomerization and evaluate the effect of reaction condition. Many methods have been developed to assess the UV-induced isomerization of such stilbenes like gas chromatography (GC) [25–28], liquid chromatography (LC) [17,29], and micellar electrokinetic chromatography (MEKC) [30]. However, the GC and LC methods require a significant amount of time and material consumption, and may result in some *trans* to *cis* isomerization during the process of treatment.

CE, which provides the determination of the yields of the UV-induced isomerization, is the fastest and less reagent consuming technique. Moreover, the effect of reaction conditions can be evaluated if the CE developed method allows their simultaneous separation and determination. Compared with traditional chromatography methods, CE has unique advantages that make it an excellent candidate for analysis of this UV-induced isomerization including, requirement of very small injection volumes (nanoliters), fast separation and high efficiency [31,32].

Besides, contamination of the stilbenes with other UV-absorbing materials (e.g., oxidation products) may result in alteration of the concentration, leading to misinterpretation of the conversion ratio of the UV-induced *cis–trans* isomerization. The reliability of CE purity analysis of *cis*- and *trans*-isomers may thus be improved con-

* Corresponding author at: Department of Chemistry, Lanzhou University, Lanzhou 730000, China. Tel.: +86 931 891 2763; fax: +86 931 891 2582.
E-mail address: chenxg@lzu.edu.cn (X. Chen).

0021-9673/$ – see front matter © 2011 Elsevier B.V. All rights reserved.
doi:10.1016/j.chroma.2011.06.100

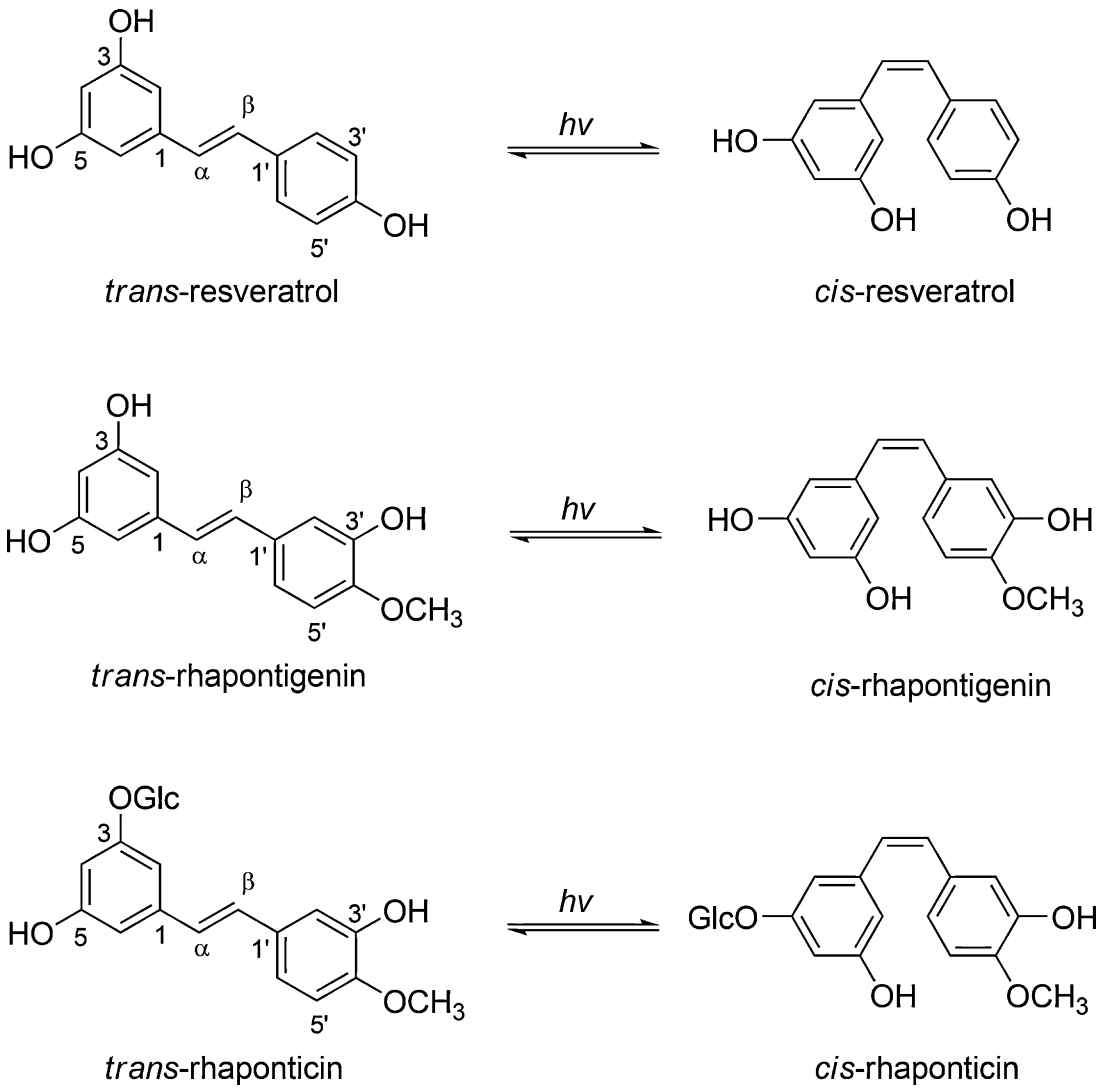

Fig. 1. UV-induced isomerizations of *trans*-resveratrol (RES), *trans*-rhapontigenin (RHA) and *trans*-rhaponticin (RHA-Glc) with the products: *cis*-resveratrol, *cis*-rhapontigenin and *cis*-rhaponticin.

siderably by checking peak purity and spectral identity by diode array detector (DAD) analysis of the spectrum.

Another routinely used approach to study the *cis–trans* isomerization of stilbenes includes the use of UV–vis spectroscopy [18]. So we also used UV–vis spectroscopy to study the effect of irradiation time and irradiation wavelength. The experimental results from UV–vis spectrum verified the feasibility of the proposed CE method for the study of UV-induced *cis–trans* isomerization.

NMR spectroscopy, even if it is a more time and reagent consuming technique, permits to obtain more information about *trans* material and *cis* product of UV-induced isomerization. First, the stereochemical characteristics of the materials and products were assessed by NMR spectroscopy which is a powerful technique and one of the main tools of research for structural investigation of molecules [33–35] as well as isomerization [36–38]. Second, CE and UV–vis techniques provide data based on the whole molecule. On the contrary, NMR spectroscopy, through the study of the variation of chemical shifts for various proton signals, allows to obtain information on the environment of individual atoms and intramolecular interactions.

To the best of our knowledge, comprehensive data describing the photochemical stability and isomerize reactivity of RHA and its glucoside RHA-Glc are scarce. Herein, the UV-induced *cis–trans* isomerization process of photosensitive stilbene compounds RHA and RHA-Glc were studied. Our objectives were to investigate the effects of different irradiation wavelengths and different irradiation time on the isomerization in order to obtain information about the product structure and confirm whether by-products exist after UV irradiation using CZE, UV–vis and NMR spectroscopy. The developed CE method is simple, fast, with less interference and accurate to study the reaction kinetics of the UV-induced isomerization of RHA and RHA-Glc whose photo-chemical kinetics have never been studied.

2. Experimental

2.1. Chemicals and reagents

Standard *trans*-rhapontigenin (*trans*-RHA) and related glucoside *trans*-rhaponticin (*trans*-RHA-Glc) were purchased from Sigma (Aldrich Chemical Co., Inc.). *cis*-isomers are not commercially available because of their instability in solid form. Their standard solutions were therefore prepared from a 100 μM aqueous solution of *trans*-isomers by UV irradiation as literature reported [39–41]. The chemical structures of studied compounds are shown in Fig. 1.

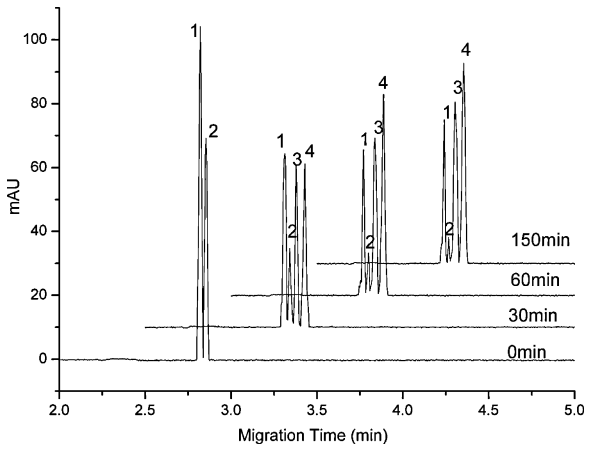

Fig. 2. Electropherograms of a standard mixture of 100 μM *trans*-RHA-Glc and 100 μM *trans*-RHA exposed to the UV lamp at 365 nm for different times. Electrophoresis conditions: 30 mM sodium tetraborate, 1 mM β-CD and 10% methanol at pH 9.0 and an applied voltage of 20 kV. (1) *trans*-RHA-Glc, (2) *trans*-RHA, (3) *cis*-RHA-Glc and (4) *cis*-RHA.

All solvents and reagents were of analytical grade and were used without further purification. Redistilled water was used throughout.

2.2. UV irradiation of the standard solution

In order to provide complete dissolution, the solid *trans*-RHA and *trans*-RHA-Glc standards (5.0 mg) were dissolved in 5.0 mL of methanol/water (50%, v:v), respectively. The solutions were stored at 4 °C. The stock solutions were diluted to certain concentration with methanol/water mixture, and then they were UV irradiated using a WFH-203 Tripurpose ultraviolet analyzer (Dark-box Triusage Ultraviolet Analysis Instrument) with UV lamp at 365 nm and 254 nm, respectively. After 0, 10, 30, 60, 90, 120, 150, 240 and 300 min, the samples were taken out and kept in dark at 4 °C until the measurement. During all subsequent steps, the samples were kept in the dark to prevent UV-isomerization of *trans*-isomers by ambient light.

2.3. Analytical method

The results of the UV-isomerization of the vinyl double bond in RHA and RHA-Glc were investigated by combination of CE-DAD, UV–vis spectroscopy and NMR method.

The instrument used for the CE-DAD analyses was a P/ACE 5510 system (Beckman, Fullerton, CA) with a diode array UV detector (190–300 nm). Data collection and analyses were performed by using P/ACE System Gold software (version 4.01) for Beckman. The separation was carried out on a 37 cm length (30 cm to the detector) × 75 μm I.D. fused-silica capillary (Handan Xinnuo Fiber Chromatogram Co., Ltd. Handan, China). The capillary was mounted on a cartridge and thermostated at 25 °C. The capillary was conditioned prior to its first use by flushing with 0.1 M NaOH for 5 min (P = 25 psi), then with water for 15 min (P = 25 psi), and finally with buffer solution for 10 min (P = 25 psi). Each day the capillary was flushed successively with NaOH (5 min, 25 psi), water (1 min, 25 psi), and then with buffer solution (3 min, 25 psi). Between each run, it was treated with water (1 min, 25 psi) and buffer solution (2 min, 25 psi). All solutions were filtered through a 0.45 μm microfilter before use. The sample solution was injected into the capillary by pressure of 0.5 psi for 5 s.

UV–vis absorption spectra were recorded using a TU-1901 double beam ultraviolet–visible spectrophotometer (Beijing, China) at room temperature, with a 1 cm path length quartz cell. The UV–vis

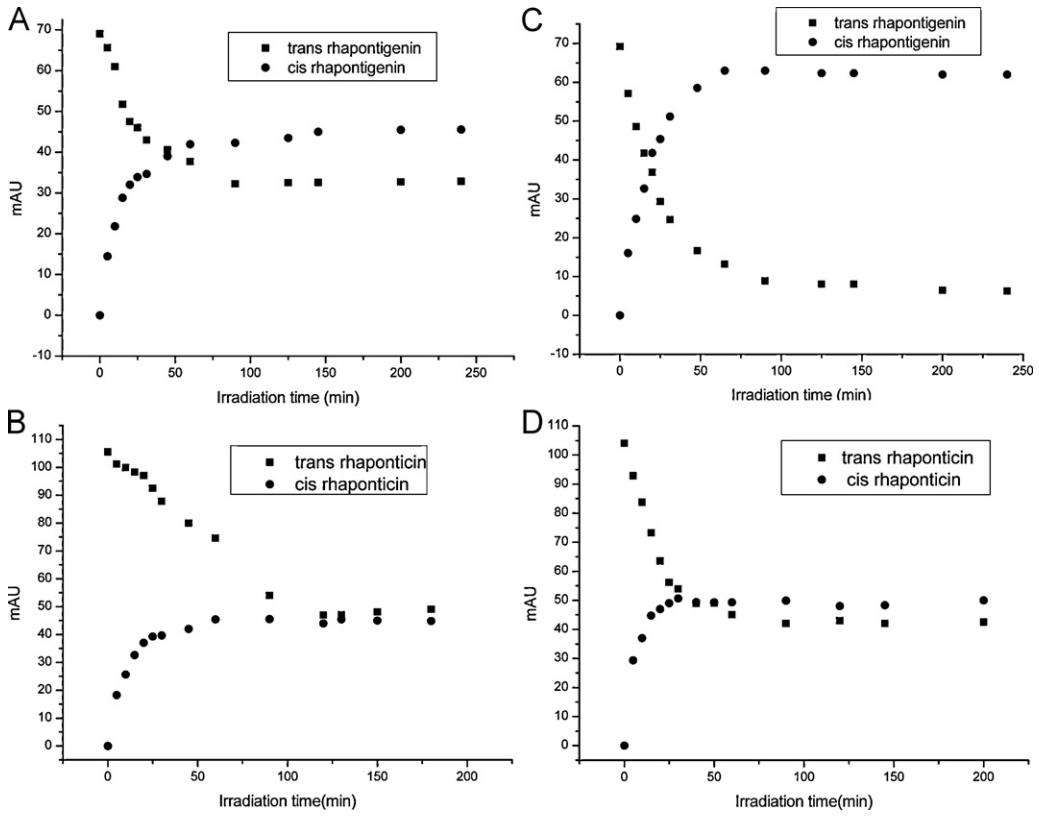

Fig. 3. (A) Isomerization curves upon irradiation of 100 μM *trans*-rhapontigenin (RHA) standard solution by UV lamp at 254 nm; (B) isomerization curves upon irradiation of 100 μM *trans*-rhaponticin (RHA-Glc) standard solution by UV lamp at 254 nm; (C) isomerization curves upon irradiation of 100 μM *trans*-rhapontigenin standard solution by UV lamp at 365 nm and (D) isomerization curves upon irradiation of 100 μM *trans*-rhaponticin standard solution by UV lamp at 365 nm.

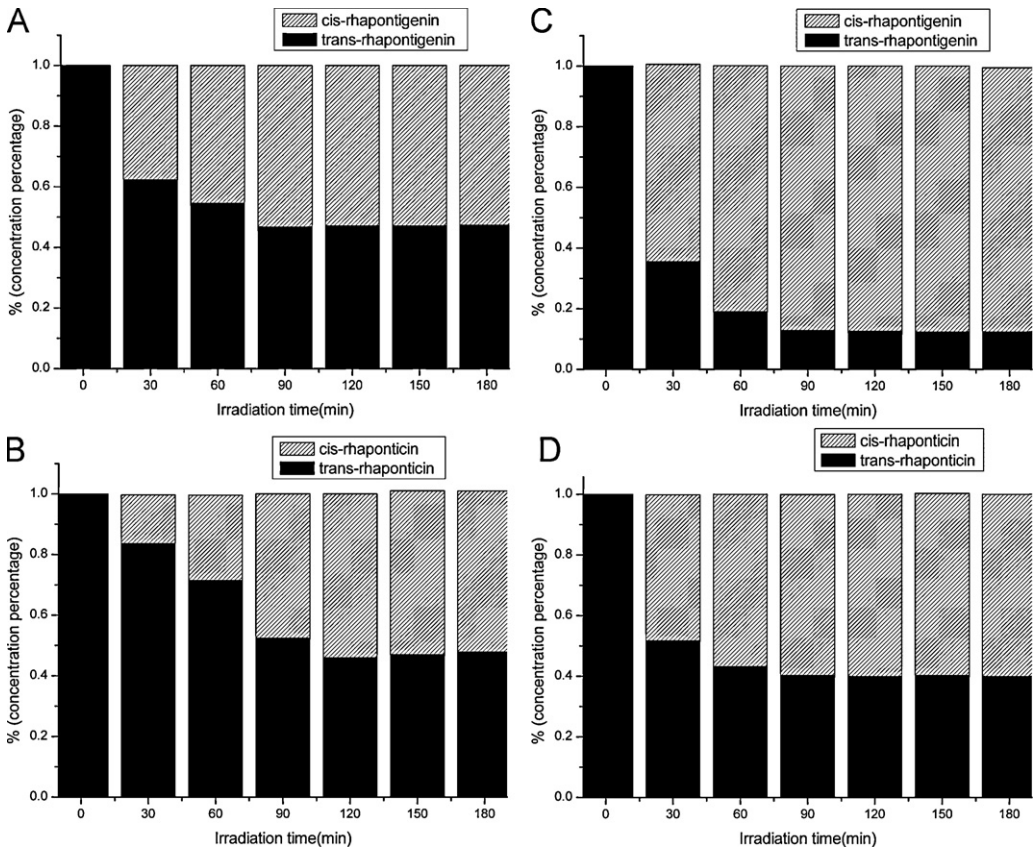

Fig. 4. *Trans*-RHA and *trans*-RHA-Glc conversion to corresponding *cis*-RHA and *cis*-RHA-Glc, change in concentration as a function of duration of UV lamp at 254 nm and 365 nm. (A) 254 nm RHA; (B) 254 nm RHA-Glc; (C) 365 nm RHA and (D) 365 nm RHA-Glc.

spectra data were applied for determination of molar absorptivity (ε) values of studied compounds.

For further structure elucidation, we performed ^{1}H and ^{13}C NMR spectroscopy of *trans*-RHA and *trans*-RHA-Glc before and after irradiation using a Bruker ARX 400 (400 MHz) spectrometer. Chemical shifts (δ) are given in ppm downfield from tetramethylsilane (TMS) as an internal standard.

2.4. Calibration

For the *trans*-isomers the calibration curves were drawn from 7 standard solutions prepared by diluting a stock solution of 100 μM *trans*-RHA and *trans*-RHA-Glc in methanol water mixture (50%, v:v), respectively. Calibration curves for *trans*- RHA and RHA-Glc were constructed separately by plotting peak areas (*y*-axis) versus concentrations (*x*-axis) of the seven standards.

For the calibration of the *cis*-isomers, decreased levels of intensity for the *trans*-isomer peaks were proportional to the area of the new peaks corresponding to the *cis*-isomer. Since no other peaks were detected under these conditions, the concentrations of *cis*-isomers were assigned on the basis of the decrease observed for *trans*-isomers.

3. Results and discussion

3.1. UV-induced isomerization revealed via β-CD modified CZE-DAD

3.1.1. Separation conditions optimization

In this section, the influence of buffer concentration, pH, CD concentration and organic modifier on the separation was optimized to achieve the best separation between the peaks of all isomers with the highest sensitivity and the shortest analysis time. In preliminary studies, a sodium tetraborate buffer was chosen as the background electrolyte and the concentration was investigated in the range of 10–40 mM. With increasing sodium tetraborate concentration, resolutions and migration times increased for all derivatives and the peak shape become poor. In order to obtain high sensitivity and keep good peak shape, a buffer of 36 mM sodium tetraborate was selected for all further experiments. The running buffer pH was noted to affect the separation efficiency and signal intensities of the isomers. The pH of running buffer was then examined from 9.0 to 9.7. As a compromise of resolution and signal intensity, pH 9.3 was chosen in subsequent experiments. However, overlapping of *cis*-, *trans*-isomer peaks was observed. As both of them exhibit similar molecular weights and charges, they are difficult to separate in normal CZE mode.

Under normal CZE conditions, these isomers cannot be separated completely, so efforts were shifted towards the use of modifiers. The addition of organic solvents to the buffer can improve the selectivity, efficiency and resolution of CE as they modified the partition coefficient, decreased viscosity, lowered the zeta potential of the capillary wall and increased selectivity [42]. Thus while separation times were longer due to the decreased electroosmosis, the resolution was greater. In our study, we investigated the effect of various organic solvents, including methanol, ethanol, acetonitril and their concentration from 5 to 30%. The experimental results showed only methanol can improve the resolution. With increasing methanol concentration, the separation efficiency improved, also, the analysis time increased due to the decreasing of the electroosmotic flow. Finally, 10% methanol was the best choice for the separation of the four *cis*-, *trans*-isomers as a compromise consideration between resolution and migration time. However, the analytes still could not be well separated.

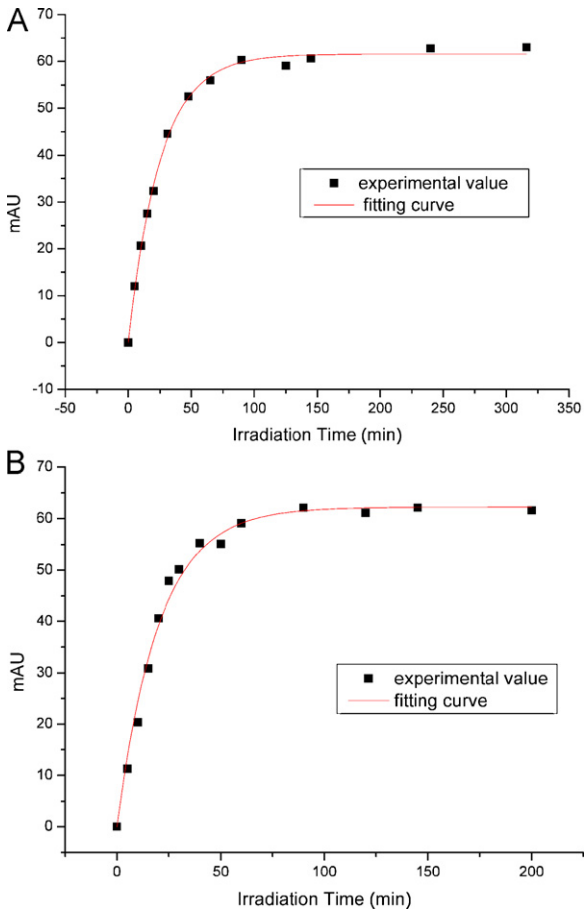

Fig. 5. (A) The change of electrophoresis signal of *trans*-RHA after irradiation of different time. (B) The change of electrophoresis signal of *trans*-RHA-Glc after irradiation of different time.

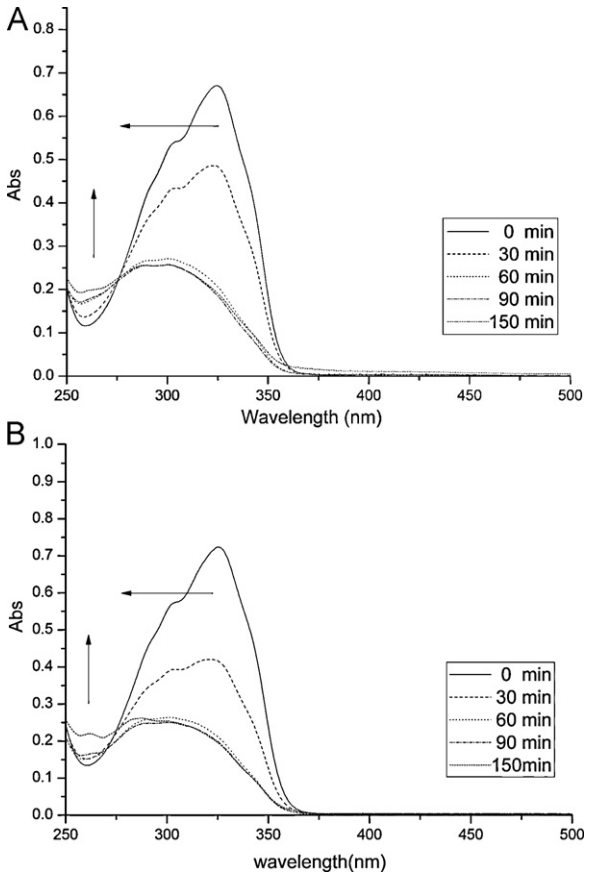

Fig. 6. Absorbance spectrums of 25 μM methanol/water solution of *trans*-RHA (A) and *trans*-RHA-Glc (B) exposed to UV lamp at 365 nm for different times (the reference was methanol/water (50%, v:v); l = 1 cm).

It has been demonstrated that complexation can considerably increase the solubility, stability and bioavailability of the guest molecule [43–45]. Furthermore, Lucas-Abellán et al. [45] reported that the size of the hydrophobic cavity of β-CDs permits stronger interactions with RES, while the hydrophobic cavity of α- and γ-CDs, is too small and too large, respectively, thus reducing their interaction with RES. So β-CD as another modifier was introduced in the subsequent experiments and the effect of concentration in the range of 0.5–5 mM on the separation was studied. The results showed that the resolution between *cis* and *trans* isomers improved with the increase in β-CD from 0.5 mM up to 1 mM, higher concentration (above 1 mM) was not beneficial to the separation of isomers. Considering the above two aspects, 1 mM β-CD was chosen in the subsequent experiments. According to the factors mentioned, the best separation was obtained with running buffer containing 30 mM sodium tetraborate, 1 mM β-CD and 10% methanol at pH 9.0 and an applied voltage of 20 kV. Under the optimized conditions, baseline separation of all four stilbenes was obtained (Fig. 2) within 3 min. It serves to illustrate the potential of CE to determine several stilbene forms.

3.1.2. Identification of peaks

These peaks identified by the following criteria: (a) the migration times were identical to the pure standard. And (b) the peak purity was confirmed by diode array analysis of the spectrum. The sample, which includes 100 μM *trans*-RHA, 100 μM *trans*- RHA-Glc was kept in the dark till measurement, only two single peaks were detected, which migrated at 2.82 min and 2.85 min as peak 1 and 2, respectively. They were identified as *trans*-RHA-Glc and *trans*-RHA (0 min, Fig. 2). After 30 min of UV irradiation at 365 nm the other two peaks appeared in the electropherogram, migrating at 2.88 min and 2.94 min as peak 3 and 4 (30 min, Fig. 2). Peak 3 was identified at *cis*-RHA-Glc. Peak 4 was identified as the *cis*-RHA. The identity of these compounds was further assessed by ^{1}H and ^{13}C NMR spectroscopy. Comparisons of the *cis*-RHA-Glc and *cis*-RHA NMR spectra were consistent with the reported data (details refer to Section 3.3).

Their effective mobilities were calculated according migration time, applied voltage, capillary total length and effective length. The effective mobilities of trans-RHA-Glc and trans-RHA were 19.75 and 19.54 cm^2/kV min, the effective mobilities of *cis*-RHA-Glc and *cis*-RHA were 19.27 and 18.94 cm^2/kV min, respectively. The effective mobilities indicated a noticeable difference in the hydrophobicities of these four compounds. The proximity of the two phenyl rings in *cis*-isomers could strengthen the weak hydrophobic interactions of *cis*-isomers with the β-CD. In the samples irradiated for 60 min and 150 min the height of these two latter peaks (*cis*-isomers) grew significantly showing a correlation with the decrease of two earlier migrating peaks (*trans*-isomers). The results showed that *cis*-isomer molecule is the only product originating from the UV-induced isomerization reaction while no other unknown peaks were detected (60, 150 min; Fig. 2).

3.1.3. Analytical calibration

The method validation including linearity, detection limits and precision was carried out using standard solutions under the optimized separation conditions. Figures of merit are summarized in Table 1. The linear relationship between the peak area and the concentration of analytes was obtained by using the correspond-

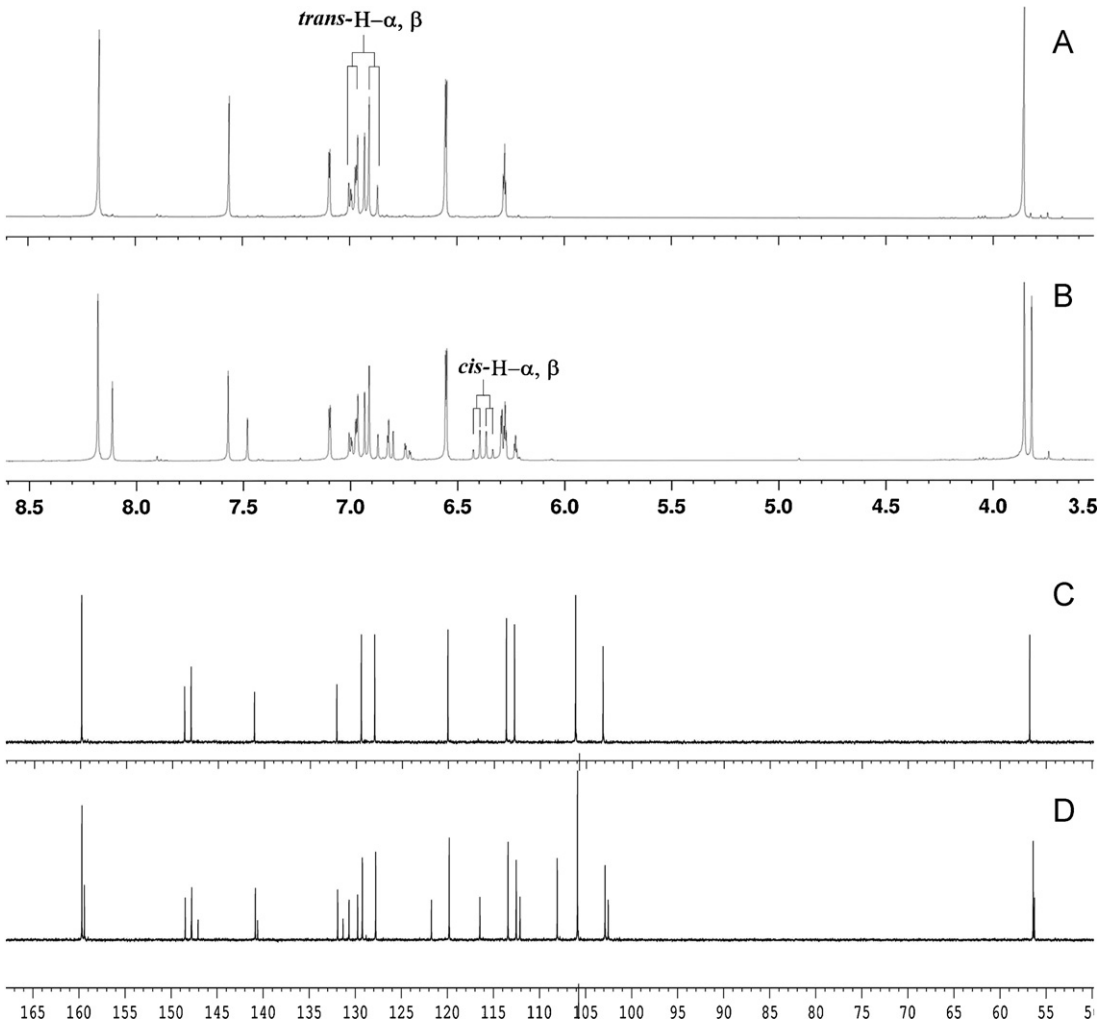

Fig. 7. (A) ^{1}H NMR (400 MHz) spectrum of initial *trans*-RHA before irradiation; (B) ^{1}H NMR (400 MHz) of the mixture of *trans*- and *cis*-RHA produced by irradiation (λ = 365 nm) with time of 5 h in acetone-d_6; (C) ^{13}C NMR (100 MHz) spectrum of initial *trans*-RHA before irradiation and (D) ^{13}C NMR (100 MHz) spectrum of the mixture of *trans*- and *cis*-RHA produced by irradiation (λ = 365 nm) with time of 5 h in acetone-d_6.

ing peak area (y) of the analytes versus their concentration (c). The results indicated that excellent linear relationship is attainable over the concentration range studied with satisfactory correlation coefficients. The detection limits, calculated for an S/N of 3, were also listed in Table 1, indicating high sensitivity. The precision of the method, including intra-day and inter-day relative standard deviations (RSD) was also listed in Table 1. The intra-day relative standard deviations of peak area were 1.4% and 1.2% at 230 nm for *trans*-isomers, and 1.7% and 1.5% at 230 nm for *cis*-isomers, indicating very high reproducibility. The limits of detection for *trans*-RHA and RHA-Glc were 0.125 and 0.116 μM at 230 nm, respectively. The limits of detection for *cis*-RHA and RHA-Glc were 0.142 and 0.134 μM at 230 nm, respectively.

3.1.4. Effect of irradiation time and wavelength

The effect of the irradiation time on the isomerization of *trans*-RHA and *trans*-RHA-Glc is shown in Fig. 3: in the first 25 min, the rate of isomerization from *trans* to *cis* was very fast. Then the responding signal of these peaks almost reached their maximum in the irradiated sample as the signals did not change significantly after 2 h, and the rate of equilibrium was different for RHA and RHA-Glc with different UV wavelength, the calculation of the rate constant was presented in Section 3.1.5 at the 365 nm wavelength, the conversion rate was obviously faster than the rate at 254 nm wavelength for both RHA and RHA-Glc (Fig. 4). From Fig. 4 we can also find that even prolonged irradiation time at both 254 nm and 365 nm, no other by-products appeared in the process of isomer-

Table 1
Calibration curves and performance characteristics of CE-DAD system.

Peak no.	Analyte	Regression equation		Correlation coefficient	Linearity (μM)	RSD (%, n = 5)				LOD (μM)
		Slope	Intercept			Intra-day		Inter-day		
						MT	PA	MT	PA	
1	Trans-RHA-Glc	3.17×10^7	3.16×10^5	0.9994	3–336	0.35	1.21	0.45	1.33	0.116
2	Trans-RHA	2.16×10^7	2.77×10^4	0.9985	3–356	0.81	1.41	1.2	1.68	0.125
3	Cis-RHA-Glc	6.41×10^7	7.48×10^4	0.9986	1–100	0.23	1.53	0.25	1.76	0.134
4	Cis-RHA	3.47×10^7	9.80×10^4	0.9932	1–100	0.67	1.72	0.7	1.85	0.142

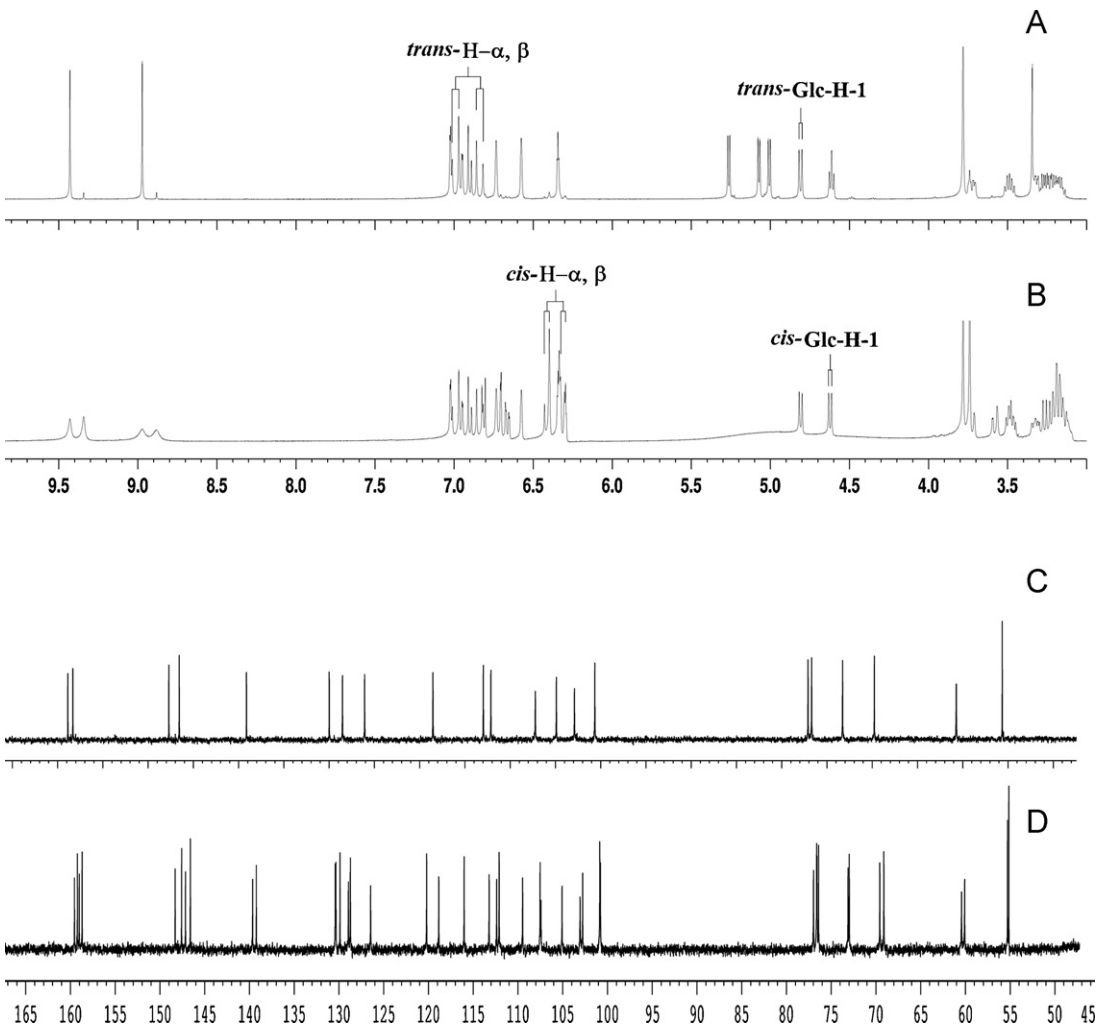

Fig. 8. (A) ^{1}H NMR (400 MHz) spectrum of initial *trans*-RHA-Glc before irradiation; (B) ^{1}H NMR (400 MHz) of the mixture of *trans*- and *cis*-RHA-Glc produced by irradiation (λ = 365 nm) with time of 5 h in DMSO-d_6; (C) ^{13}C NMR (100 MHz) spectrum of initial *trans*-RHA-Glc before irradiation and (D) ^{13}C NMR (100 MHz) spectrum of the mixture of *trans*- and *cis*-RHA-Glc produced by irradiation (λ = 365 nm) with time of 5 h in DMSO-d_6.

ization and 100% of the peak areas accounted for all of the initial *trans*-isomer, the *trans*-reactant converted to *cis*-product in proportion. On the other hand, Trela and Waterhouse [17] reported that the isomerization yield of RES was highly variable, and depended on the UV wavelength (10% versus 90% after 1 h irradiation at 254 and 366 nm, respectively). We can observe that equilibrium was achieved with a larger final conversion ratio at 365 nm (Fig. 4C and D) than at 254 nm (Fig. 4A and B) for both *trans*-RHA and *trans*-RHA-Glc. The results were consistent with the phenomena reported in the literature [17]. The data confirmed that the effect of 365 nm UV light was greater than that of 254 nm UV light on the isomerization rate and conversion ratio.

The use of natural UV from sunlight for isomerization is probably less efficient than exposure to an UV lamp and the exact equilibrium rate of *cis*-, *trans*-isomer mixture may depend on the specific spectrum of light reaching the sample. In the experiment where 10 min to 5 h of UV irradiation was applied, no any other by-product was detected which was further confirmed in the next UV–vis and NMR assay.

3.1.5. Calculation of reaction rate

The *cis*–*trans* isomerization of *trans*-RHA after irradiation of UV light can be described as follow equation:

$$\textit{trans}\text{-RHA} \xrightarrow{k} \textit{cis}\text{-RHA} \quad (1)$$

The rate of this reaction is directly proportional to the concentration of *trans*-RHA. If c_t is the concentration of the reactant *trans*-RHA at any time *t*, the rate of disappearance of *trans*-RHA can be expressed mathematically as

$$\frac{-dc_t}{dt} = kc_t \quad (2)$$

where *k* is proportionality constant called the specific reaction rate constant for the first order rate equation.

Calculating indefinite integral

$$\Delta c_t = \Delta c_{\max}(1 - e^{-kt}) \quad (3)$$

Here, Δc_t, $\Delta c_{\max}$ were the varied concentrations of *trans*-RHA at time *t* and $t \to \infty$ (means reaction reach equilibrium). Besides, with the increase of Δc, the signal response of *trans*-RHA in electropherogram was increased. Δc is proportional to ΔA, so we get the following equation:

$$\Delta A_t = \Delta A_{\max}(1 - e^{-kt}) \quad (4)$$

Here, ΔA_t and $\Delta A_{\max}$ were the variations of signal response of *trans*-RHA in electropherogram at time *t* and $t \to \infty$, respectively. $\Delta A_{\max}$ and *k* could be obtained by fitting the experimental data according to Eq. (4), the result shown in Fig. 5(A) and (B). It can be seen the fitting results fitted very well with the experimental data. And the $\Delta A_{\max}$ was 61.5, the reaction rate constant *k* was

0.0397 min^{-1}. Use the same method, we calculated the ΔA_{max} for *trans*-RHA-Glc was 62.2, and the reaction rate constant *k* for *trans*-RHA-Glc was 0.0498 min^{-1}.

3.2. UV-induced isomerization revealed via UV–vis spectroscopy

In order to investigate the photoconversion process, we also measured the UV–vis spectra of trans isomers before and after exposure to UV-light. The UV–vis spectra properly represented the process of the UV-induced isomerization, and compared the phenomenon with that observed in CE system to validate the feasibility of CE-DAD system for the study of *cis–trans* isomerization. The test solution containing 25 μM of pure *trans*-isomer was sealed in a quartz tube and irradiated for different times (0, 10, 60, 120 and 240 min) at 365 nm selected from a UV lamp. Fig. 6 shows the UV–vis spectra of *trans*-RHA and *trans*-RHA-Glc, measured after different exposure times. After a 2 h exposure to light, the absorption of the RHA solution at 325 nm decreased by more than 60%. In addition, as shown in Fig. 6A, there was a clearly visible shift in the maximum absorption wavelength from 325 to 288 nm, together with an increase in the absorbance at 260 nm. As noted obviously, 286 nm should be reported as the maximum absorption wavelength of *cis*-RHA. Similar UV spectra for RHA-Glc were found with the absorption at 325 nm decreased by more than 64%, and similar blue shift was observed from 325 to 288 nm (Fig. 6B). The molar absorptivity was 36824 L mol^{-1} cm^{-1} at λ_{max} 324.5 nm for *trans*-RHA and 43894 L mol^{-1} cm^{-1} at λ_{max} 325 nm for *trans*-RHA-Glc.

3.3. Structure identification of the isomerization compound via NMR spectroscopy

To establish the UV light induced alteration of the proton chemical shifts in the molecule of the *cis–trans* isomerization of the double bond, further ^{1}H NMR spectra in deuterated reagents throughout the UV light irradiation have been acquired and *cis*/*trans* equilibrium has been determined as a function of irradiation time.

10 mg *trans*-RHA and 10 mg *trans*-RHA-Glc were dissolved in 0.5 mL of acetone-d_6 and DMSO-d_6 in 5 mm NMR tubes, respectively. Both samples were irradiated with a 365 nm UV lamp for 5 h, respectively. After irradiation, each mixture was then taken NMR measurements directly.

^{1}H and ^{13}C NMR spectra of both samples showed doubling of all resonance signals and the existence of a mixture of isomeric forms (*cis* and *trans* forms) of RHA (Fig. 7) and RHA-Glc (Fig. 8) in agreement with the CE-DAD method. The stereochemical features of the two stilbenes and the distinguish of the olefinic proton signals of the two isomeric forms have been established by means of the proton spin–spin coupling constants extracted by analysis of the ^{1}H NMR spectra.

The protons signals of the CH=CH group and those of the aromatic ring in the *cis* form were shifted upfield due to the difference in molecular conformation of the *trans* form and higher shielding. The chemical shifts of the α- and β-protons are more sensitive to the conformational transformations of the double bond when compared to the aromatic protons. These NMR data implied the occurrence of a stronger steric interaction in *cis*-isomers than in *trans*-isomers. In the ^{1}H NMR spectrum of *trans*-RHA-Glc, two olefinic proton signals appeared at δ 6.84 (1H, d, *J* = 16.0 Hz, H-α), 6.99 (1H, d, *J* = 16.0 Hz, H-β), whose coupling constant suggested the presence of a *trans*-olefinic group, while for the corresponding *cis*-RHA-Glc, a pair of comparatively high field doublets (δ 6.32, 6.42) with coupling constant of 12.0 Hz was recorded. Similarly, in the ^{1}H NMR spectrum of *trans*-RHA, the olefinic proton signals appeared at δ 6.89 (1H, d, *J* = 16.4 Hz, H-α), and 6.99 (1H, d, *J* = 16.4 Hz, H-β), while in the *cis*-RHA, both the olefinic protons were shifted upfield (δ 6.32, 6.42) with coupling constant of 12.0 Hz. Spectral data of both *cis*-, *trans*-isomers of RHA and RHA-Glc obtained are in agreement with those previously reported [46–48]. The detailed ^{1}H and ^{13}C NMR spectra data of *cis*-, *trans*-RHA and RHA-Glc are presented in the Supplementary data.

4. Conclusions

A new, rapid and sensitive CE method investigating the kinetics of UV-induced *cis–trans* isomerization of RHA and RHA-Glc isomers under UV irradiation with different wavelength and exposure time was developed. The quantitative analysis of the UV-induced *cis–trans* isomerization of the four stilbene compounds was easily achieved with high accuracy and efficiency. The reaction rate constants were calculated for both RHA and RHA-Glc. Furthermore, the process of the UV-induced isomerization was studied using UV–vis spectrum, and the result was consistent with that of the CE system. They both showed that the *trans*-reactant converted into *cis*-product in proportion with no other by-product. This work illustrates the potential application of CE for the study of kinetics of UV-induced isomerization of other photosensitive compounds. Compared to traditional methods for the study of kinetics, the proposed system combined the superiorities of CE and UV–vis spectroscopy and made the kinetic study more simple, fast and accurate.

The method has potential for use in the identification of *in vitro* and *in vivo* samples which contain these photosensitive compounds. It will permit new investigation into the biological activities of these antioxidants at different ambiguous light environment. Finally, knowledge of the photochemistry behavior of *trans*-RHA and RHA-Glc at different irradiation conditions is of great importance for the pharmaceutical industry because of the growing interest in developing medicines or healthy food enriched with these natural antioxidants.

Acknowledgment

This work was kindly supported by the National Natural Science Foundation of China (No. 20875040).

Appendix A. Supplementary data

Supplementary data associated with this article can be found, in the online version, at doi:10.1016/j.chroma.2011.06.100.

References

[1] A. Aaviksaar, M. Haga, K. Kuzina, T. Püssa, A. Raal, G. Tsoupras, Proc. Estonian Acad. Sci. Chem. 52 (2003) 99.
[2] N. Rupprich, H. Hildebrand, H. Kindl, Arch. Biochem. Biophys. 200 (1980) 72.
[3] E.K. Park, M.K. Choo, H.K. Yoon, D.H. Kim, Arch. Pharm. Res. 25 (2002) 528.
[4] H.L. Li, A.B. Wang, Y. Huang, D.P. Liu, C. Wei, G.M. Williams, C.N. Zhang, G. Liu, Y.Q. Liu, D.L. Hao, R.T. Hui, M. Lin, C.C. Liang, Free Radical Biol. Med. 38 (2005) 243.
[5] A. Raal, P. Pokk, A. Arend, M. Aunapuu, J. Jõgi, K. Õkva, T. Püssa, Phytother. Res. 23 (2009) 525.
[6] S. Ulrich, F. Wolter, J.M. Stein, Mol. Nutr. Food Res. 49 (2005) 452.
[7] I. Rahman, S.K. Biswas, P.A. Kirkham, Biochem. Pharmacol. 72 (2006) 1439.
[8] F. Orallo, Curr. Med. Chem. 13 (2006) 87.
[9] M. Campos-Toimil, J. Elies, E. Alvarez, I. Verde, F. Orallo, Eur. J. Pharmacol. 577 (2007) 91.
[10] M. Yanez, N. Fraiz, E. Cano, F. Orallo, Biochem. Biophys. Res. Commun. 344 (2006) 688.
[11] J.P. Basly, F. Marre-Fournier, J.C. Le Bail, G. Habrioux, A.J. Chulia, Life Sci. 66 (2000) 769.
[12] M. Heger, B.M. Ventskovskiy, I. Borzenko, K.C. Kneis, R. Rettenberger, M. Kaszkin-Bettag, P.W. Heger, Menopause 13 (2006) 744.
[13] E. Ignatowicz, W. Baer-Dubowska, Pol. J. Pharmacol. 53 (2001) 557.
[14] J. Leiro, E. Alvarez, J.A. Arranz, R. Laguna, E. Uriarte, F. Orallo, J. Leukoc. Biol. 75 (2004) 1156.
[15] C.A. de la Lastra, I. Villegas, Biochem. Soc. Trans. 35 (2007) 1156.

[16] S. Hassan-Khabbar, C.H. Cottart, D. Wendum, F. Vibert, J.P. Clot, J.F. Savouret, M. Conti, V. Nivet-Antoine, Liver Transpl. 14 (2008) 451.
[17] B.C. Trela, A.L. Waterhouse, J. Agric. Food Chem. 44 (1996) 1253.
[18] L. Camont, C.H. Cottart, Y. Rhayem, V. Nivet-Antoine, R. Djelidi, F. Collin, J.L. Beaudeux, D. Bonnefont-Rousselot, Anal. Chim. Acta 634 (2009) 121.
[19] Y.L. Jiang, Bioorg. Med. Chem. 16 (2008) 6406.
[20] J.M. López-Nicolas, F. García-Carmona, J. Agric. Food Chem. 56 (2008) 7600.
[21] C.H. Lin, Y.H. Chen, Electrophoresis 22 (2001) 2574.
[22] V. Brandolini, A. Maietti, P. Tedeschi, E. Durini, S. Vertuani, S. Manfredini, J. Agric. Food Chem. 50 (2002) 7408.
[23] R. Montes, M. García-López, I. Rodríguez, R. Cela, Anal. Chim. Acta 673 (2010) 47.
[24] T.G. Luan, G.K. Li, M.Q. Zhao, Z.X. Zhang, Anal. Chim. Acta 424 (2000) 19.
[25] H.E. Siemann, L.L. Creasy, Am. J. Enol. Viticult. 43 (1992) 49.
[26] D.M. Goldberg, J. Yan, E. Ng, E.P. Diamandis, A. Karumanchiri, G. Soleas, A.L. Waterhouse, Anal. Chem. 66 (1994) 3959.
[27] G. Soleas, D.M. Goldberg, E.P. Diamandis, A. Karumanchiri, J. Yan, E. Ng, Am. J. Enol. Viticult. 46 (1995) 346.
[28] O. Lamikanra, C.C. Grime, J.B. Rodin, I.D. Inyang, J. Agric. Food Chem. 44 (1996) 1111.
[29] J.S. Jensen, C.F. Wertz, V.A. O'Neill, J. Agric. Food Chem. 58 (2010) 1685.
[30] Q.Y. Chu, M. O'Dwyer, M.G. Zeece, J. Agric. Food Chem. 46 (1998) 509.
[31] M.G. Zeece, Trends Food Sci. Technol. 3 (1992) 6.
[32] C.A. Hall, A. Zhu, M.G. Zeece, J. Agric. Food Chem. 42 (1994) 919.
[33] J.N.S. Evans, Biomolecular NMR Spectroscopy, 1st ed., Oxford University Press, 1995.
[34] Q. Teng, Structural Biology: Practical NMR Applications, Springer, NY, 2005.
[35] C.A. Evans, D.L. Rabenstein, J. Am. Chem. Soc. 96 (1974) 7312.
[36] S. Bouabdallah, H. Trabelsi, T.B. Dhia, S. Sabbah, K. Bouzouita, R. Khaddar, J. Pharm. Biomed. Anal. 31 (2003) 731.
[37] V.V. Syakaev, S.N. Podyachev, B.I. Buzykin, Sh.K. Latypov, V.D. Habicher, A.I. Konovalov, J. Mol. Struct. 788 (2006) 55.
[38] S.P. Babailov, Prog. Nucl. Magn. Reson. Spectrosc. 54 (2009) 183.
[39] D.M. Goldberg, E. Ng, A. Karumanchiri, J. Yan, E.P. Diamandis, G.J. Soleas, J. Chromatogr. A 708 (1995) 89.
[40] X.J. Chen, H. He, G.J. Wang, B. Yang, W.C. Ren, L. Ma, Q.L. Yu, Biomed. Chromatogr. 21 (2007) 257.
[41] D. Blache, I. Rustan, P. Durand, G. Lesgards, N. Loreau, J. Chromatogr. B: Biomed. Sci. Appl. 702 (1997) 103.
[42] T.K. McGhie, K.R. Markham, Phytochem. Anal. 5 (1994) 121.
[43] E.M. Martin Del Valle, Process Biochem. 39 (2004) 1033.
[44] Y. Cai, S.H. Gaffney, T.H. Lilley, D. Magnolato, R. Martin, C.M. Spencer, E. Haslam, J. Chem. Soc. Perkin Trans. 2 (1990) 2197.
[45] C. Lucas-Abellán, M.I. Fortea, J.A. Gabaldón, E. Núñez-Delicado, Food Chem. 111 (2008) 262.
[46] T.A. Aburjai, Phytochemistry 55 (2000) 407.
[47] M. Roberti, D. Pizzirani, D. Simoni, R. Rondanin, R. Baruchello, C. Bonora, F. Buscemi, S. Grimaudo, M. Tolomeo, J. Med. Chem. 46 (2003) 3546.
[48] Y. Kashiwada, G. Nonaka, I. Nishioka, Chem. Pharm. Bull. 32 (1984) 3501.